Progress In Electromagnetics Research, PIER 21, 71–89, 1999

ANALYSIS OF SCATTERING FROM PERFECTLY CONDUCTING PLATES BY THE USE OF AMMM

C. Su

Dept. of Applied Math.
Northwestern Polytechnical University
Xian, Shaanxi, P.R. China

T. K. Sarkar

Dept. of Electrical and Computer Engineering
Syracuse University
Syracuse, NY 13244, U.S.A

1. INTRODUCTION

Electromagnetic scattering from thin arbitrary shaped perfectly conducting plates is of interest and importance. The moment method is one of the most popular numerical techniques that exist for its flexibility to analyze the scattering and radiation from the complex geometries. It has been in use over the past thirty years [1,2]. When the size of scatterers or radiators is electrically large even resonant, the moment method becomes computationally too expensive (too much memory and CPU time) to analyze them.

In order to overcome the difficulty of the moment method, many types of hybrid techniques which is based on high-frequency techniques and low-frequency techniques have been proposed. The review of these hybrid

techniques can been found in [3–5]. Although these hybrid techniques can deal with many scattering and radiating from complex objects, they cannot solve the problem of electrically large complex objects with a high degree of accuracy. Recently, many researchers tried to solve directly these large computationally intensive problems by the combination of the conventional MoM and other new techniques because the conventional MoM matrix contains all of the information required to solve a scattering or radiating problems. In these new techniques, there are the impedance matrix localization method (IML) [6–9], the fast multipole method (FMM) [10–12], the complex multipole beam approach (CMBA) [13], the matrix decomposition algorithm (MDA) [14], and its multilevel cousin: a multilevel matrix decomposition algorithm (MLMDA) [15–16], etc. Reference [17] provides a detail discussion of these fast solution methods for efficiently solving electromagnetic problems.

Another method is the adaptive multiscale moment method (AMMM) proposed by the authors [18–20]. A special kind of multiscale basis functions on a bounded interval has been introduced, which is similar to a wavelet-like basis functions, in order to solve the Fredholm integral equation of the first-kind in one dimension. From the previous papers on AMMM, we know that AMMM possesses three characteristics: (1) The moment matrix on the multiscale basis has to be computed directly from the original moment matrix utilizing the triangular basis through a basis transformation matrix. (2) When the scale is increased, the initial guess for the solution utilized in an iterative solver at the new scale, corresponds to the solution of the original scale. (3) The size of the linear equations can be automatically reduced through filtering the small coefficient terms by a priori threshold. Although AMMM is based on solving the one-dimensional integral equation, the method can be applied to solving the two- or three-dimension integral equation from the point of view of solving the linear equation by the matrix transformation. Our motivation in the present paper is to apply AMMM to analyze scattering by thin, perfectly conducting plates in the three dimensions.

Since the mid 1970's, several researchers have proposed different methods for analyzing the full three-dimensional electromagnetic scattering problem for a perfectly conducting plate. One method directly discretized the integral equation by use of the moment method [21–23]. Another type of method is to first use Fourier transform to deal with the spatial derivation of the grad-div operation of the hyper-singular integral equation, and then discretize the integral equation in the spectral Fourier domain. Lastly linear equations are solved by the conjugate gradient method which has only an $O(N)$ memory requirement. This method is called (CG-FFT [24–28]. In

all of these approaches, different types of basis functions have been chosen: [21–25,27] which have adopted the pulse basis for both expansion and testing functions, where as [26,28] adopted the rooftop functions as expansion and testing functions which can yield more accurate results at an increased computational costs.

This paper focuses on analyzing the scattering from perfectly conducting plates by AMMM. Section 2 directly discretizes the integral equation based on the pulse basis by the use of the moment method. The impedance matrix and the source terms are then obtained based on a five-point average point- matching scheme. Section 3 discusses the AMMM to solve the linear equation discretized from the integral equation. Section 4 presents some numerical examples for analyzing scattering from the perfectly conducting rectangular plates.

2. THE CONVENTIONAL MONENT METHOD

Let S denote the surface of an arbitrary perfectly conducting plate in the xy plane. Let $\vec{E}^i$ be the electric field, defined by an impressed source in the absence of the scatterer. The field is incident on the structure and induces surface currents $\vec{J}$ on S. The scattered electric field $\vec{E}^s$ can be computed from the surface currents by:

$$\vec{E}^s(\vec{r}) = -j\omega\vec{A}(\vec{r}) - \nabla\phi(\vec{r}) \tag{1}$$

with the magnetic vector potential defined by

$$\vec{A}(\vec{r}) = \frac{\mu}{4\pi}\int\limits_S \vec{J}(\vec{r}')\frac{\exp(-jkR)}{R}ds' \tag{2}$$

and the scalar potential as

$$\phi(\vec{r}) = \frac{1}{4\pi\varepsilon}\int \nabla\cdot\vec{J}(\vec{r}')\frac{\exp(-jkR)}{R}ds' \tag{3}$$

A harmonic time dependence according to $\exp(j\omega t)$ is assumed and is suppressed for conveniences, and $k = \omega\sqrt{\mu\varepsilon} = 2\pi/\lambda$, where λ is the wavelength.

We can define an integro-differential equation for $\vec{J}$ by applying the boundary condition $\hat{n}\times(\vec{E}^i + \vec{E}^s) = \hat{0}$ on the surface S, obtaining the following equation (EFIE)

$$-\vec{E}(\vec{r})|_{\tan} = [-j\omega\vec{A}(\vec{r}) - \nabla\phi(\vec{r})|_{\tan} \quad \vec{r} \text{ on } S \tag{4}$$

Because the surface of S is an arbitrary plate in the xy plane, the induced current $\vec{J}$ can be written as

$$\vec{J}(\vec{r}) = J_x(\vec{r})\hat{x} + J_y(\vec{r})\hat{y} \tag{5}$$

Therefore, (4) can be rewritten in the following form

$$\begin{cases} \dfrac{jk\eta_0}{4\pi} \displaystyle\int_s [L_{11}(GJ_x) + L_{12}(GJ_y)]\, ds' = E_x^i \\ \dfrac{jk\eta_0}{4\pi} \displaystyle\int_s [L_{12}(GJ_x) + L_{22}(GJ_y)]\, ds' = E_y^i \end{cases} \tag{6}$$

where

$$L_{11} = 1 + \frac{1}{k^2}\frac{\partial^2}{\partial x^2}, \qquad L_{12} = \frac{1}{k^2}\frac{\partial^2}{\partial x \partial y}, \qquad L_{22} = 1 + \frac{1}{k^2}\frac{\partial^2}{\partial y^2},$$

$$G = \frac{\exp\left[-jk\sqrt{(x-x')^2 + (y-y')^2}\right]}{\sqrt{(x-x')^2 + (y-y')^2}},$$

$$\vec{E}^i = (E_\theta \hat{\theta} + E_\varphi \hat{\varphi}) \exp\left[jk(x\sin\theta\cos\varphi + y\sin\theta\sin\varphi)\right]$$

$$E_x^i = \hat{x}\cdot\vec{E}^i, \qquad E_y^i = \hat{y}\cdot\vec{E}^i.$$

Suppose the plate S is divided into a set of small rectangular plates $\{s_n\}$, $\vec{r}_n = (x_n, y_n)$ is the centroid of the cell s_n, whose length and width are $2\Delta x_n$, $2\Delta y_n$.

The unknown currents J_x, J_y are expanded by the pulse function on $\{s_n\}$ and the point marching carried out at the centroid (x_n, y_n) of the cell s_n is performed through the conventional moment method, which gives rise to the following matrix equation

$$\begin{pmatrix} A_{11} & A_{12} \\ A_{12} & A_{22} \end{pmatrix} \begin{pmatrix} \overline{J}_x \\ \overline{J}_y \end{pmatrix} = \frac{4\pi}{jk\eta_0} \begin{pmatrix} \overline{E}_x^i \\ \overline{E}_y^i \end{pmatrix} \tag{7}$$

where

$$A_{11}(i,j)=\int\limits_{s_j} L_{11}(G|_{(x_i,y_i)})ds';\qquad A_{12}(i,j)=\int\limits_{s_j} L_{12}(G|_{(x_i,y_i)})ds';$$

$$A_{22}(i,j)=\int\limits_{s_j} L_{22}(G|_{(x_i,y_i)})ds'\qquad (i=1,2,\ldots,N,\ j=1,2,\ldots,N)$$

$$\overline{J}_x=(J_x(\vec{r}_1),\cdots,J_x(\vec{r}_N))',\qquad \overline{J}_y=(J_y(\vec{r}_1),\cdots,J_y(\vec{r}_N))'$$
$$\overline{E}^i_x=\big(E^i_x(\vec{r}_1),\cdots,E^i_x(\vec{r}_N)\big)',\quad \overline{E}^i_y=\big(E^i_y(\vec{r}_1),\cdots,E^i_y(\vec{r}_N)\big)'$$

$$\begin{aligned}A_{12}(i,j)=&\frac{1}{k^2}\Big(G(x_j+\Delta x_j-x_i,y_j+\Delta y_j-y_i)\\&-G(x_j-\Delta x_j-x_i,y_j+\Delta y_j-y_i)\\&-G(x_j+\Delta x_j-x_i,y_j-\Delta y_j-y_i)\\&+G(x_j-\Delta x_j-x_i,y_j-\Delta y_j-y_i)\Big)\end{aligned}$$

$$\begin{aligned}\int\limits_{s_j} G|_{(x_i,y_i)}ds'=&\frac{\Delta x_j\Delta y_j}{9}\Big[G(x_j-\Delta x_j-x_i,y_j-\Delta y_j-y_i)\\&+4G(x_j-x_i,y_j-\Delta y_j-y_i)\\&+G(x_j+\Delta x_j-x_i,y_j-\Delta y_j-y_i)\\&+4G(x_j-\Delta x_j-x_i,y_j-y_i)+16G(x_j-x_i,y_j-y_i)\\&+4G(x_j+\Delta x_j-x_i,y_j-y_i)\\&+G(x_j-\Delta x_j-x_i,y_j+\Delta y_j-y_i)\\&+4G(x_j-x_i,y_j+\Delta y_j-y_i)\\&+G(x_j+\Delta x_j-x_i,y_j+\Delta y_j-y_i)]\qquad (j\neq i)\end{aligned}$$

$$\begin{aligned}\int\limits_{s_i} G|_{(x_i,y_i)}ds'=&\int\limits_{-\Delta y_i}^{\Delta y_i}dy\int\limits_{-\Delta x_i}^{\Delta x_i}\frac{\exp\left[-jk\sqrt{x^2+y^2}\right]}{\sqrt{x^2+y^2}}dx\\=&\int\limits_0^{2\pi}d\theta\int\limits_0^{r^*}\frac{\exp[-jkr]}{r}rdr\\=&2\pi\frac{1-\exp[-jkr^*]}{jk},\qquad r^*=2\sqrt{\frac{\Delta x_i\Delta y_i}{\pi}},\quad i=j\end{aligned}$$

$$\int_{x_j} \left.\frac{\partial^2 G}{\partial x'^2}\right|_{(x_i,y_i)} ds' = \int_{y_j-\Delta y_j}^{y_j+\Delta y_j} dy' \left[\frac{\partial G}{\partial x'}\right]\Bigg|_{x_j-\Delta x_j}^{x_j+\Delta x_j}$$

$$= \int_{y_j-\Delta y_j}^{y_j+\Delta y_j} \left[\frac{x_i - x'}{R^3}(1+jkR)\exp(-jkR)\right]\Bigg|_{x'=x_j-\Delta x_j}^{x=x_j+\Delta x_j} dy'$$

$$R = \sqrt{(x'-x_i)^2 + (y'-y_i)^2} \qquad i \neq j$$

$$\int_{s_i} \left.\frac{\partial^2 G}{\partial x'^2}\right|_{(x_i,y_i)} ds' = \int_{y_i-\Delta y_i}^{y_i+\Delta y_i} \left[\frac{x_i - x'}{R^3}(1+jkR)\exp(-jkR)\right]\Bigg|_{x'=x_i-\Delta x_i}^{x'=x_i+\Delta x_i} dy'$$

$$= -4\int_0^{\Delta y_i} \frac{\Delta x_i}{\Delta x_i^2 + y^2}\left(\frac{1}{\sqrt{\Delta x_i^2 + y^2}} + jk\right)$$

$$\cdot \exp\left[-jk\sqrt{\Delta x_i^2 + y^2}\right] dy \qquad i = j$$

$$\int_{s_j} \left.\frac{\partial^2 G}{\partial y'^2}\right|_{(x_i,y_i)} ds' = \int_{x_j-\Delta x_j}^{x_j+\Delta x_j} dx' \left[\frac{\partial G}{\partial y'}\right]\Bigg|_{y_j-\Delta y_j}^{y_j+\Delta y_j}$$

$$= \int_{x_j-\Delta x_j}^{x_j+\Delta x_j} \left[\frac{y_i - y'}{R^3}(1+jkR)\exp(-jkR)\right]\Bigg|_{y'=y_j-\Delta y_j}^{y=y_j+\Delta y_j} dx'$$

$$R = \sqrt{(x'-x_i)^2 + (y'-y_i)^2} \qquad i \neq j$$

$$\int_{s_i} \left.\frac{\partial^2 G}{\partial y'^2}\right|_{(x_i,y_i)} ds' = \int_{x_i-\Delta x_i}^{x_i+\Delta x_i} \left[\frac{y_i - y'}{R^3}(1+jkR)\exp(-jkR)\right]\Bigg|_{y'=y_i-\Delta y_i}^{y'=y_i+\Delta y_i} dx'$$

$$= -4\int_0^{\Delta x_i} \frac{\Delta y_i}{\Delta y_i^2 + x^2}\left(\frac{1}{\sqrt{\Delta y_i^2 + x^2}} + jk\right)$$

$$\cdot \exp\left[-jk\sqrt{\Delta y_i^2 + x^2}\right] dx \qquad i = j$$

The radar cross section (RCS) can be shown to have the following form

$$\sigma(\theta,\phi) = \frac{k^2\eta_0^2}{4\pi}\left[\left|\sum_{n=1}^{n}\left(J_{x,n}\cos\theta\cos\phi + J_{y,n}\cos\theta\sin\phi\right)\right)\zeta(\theta,\phi,n)\right|^2 + \left|\sum_{n=1}^{n}\left(-J_{x,n}\sin\phi + J_{y,n}\cos\phi\right)\zeta(\theta,\phi,n)\right|^2\right] \tag{8}$$

where $\zeta(\theta,\phi,n) = \exp[jk\sin\theta(x_n\cos\phi + y_n\sin\phi)]$.

When one takes only the point-matching value at the centroid, the computational accuracy, in general, is not very good. So in this paper, we take the average of five point matched values in the cell to construct the impedance matrix and the source terms. The five points are the centroid point (x_n, y_n) and $(x_n \pm \frac{1}{2}\Delta x_n, y_n \pm \frac{1}{2}\Delta y_n)$.

3. ADAPTIVE MULTISCALE ALGORITHM

3.1 Adaptive Multiscale Moment Method

A brief description of the adaptive multiscale moment method is provided to illustrate on how to solve the first-kind Fredholm integral equation

$$\int_0^1 K(u,v)X(v)dv = g(u) \qquad u \in [0,1] \tag{9}$$

Detailed computational derivation may be found in [18, 19].

In the conventional moment method, the triangular basis functions $\{\varphi_i(u)\}$ are taken as expansion functions and testing functions. The above integral equation can be transformed into the following matrix equation

$$AX = B \tag{10}$$

where

$$A = \{a_{i,j}\}_{N\times N}, \quad B = (b_1, b_2, \ldots, b_N), \qquad X = (x_1, x_2, \ldots, x_N)$$

$$a_{i,j} = \int_0^1 \varphi_j(u)du \int_0^1 K(u,v)\varphi_i(v)dv, \qquad b_j = \int_0^1 \varphi_j(u)g(u)du$$

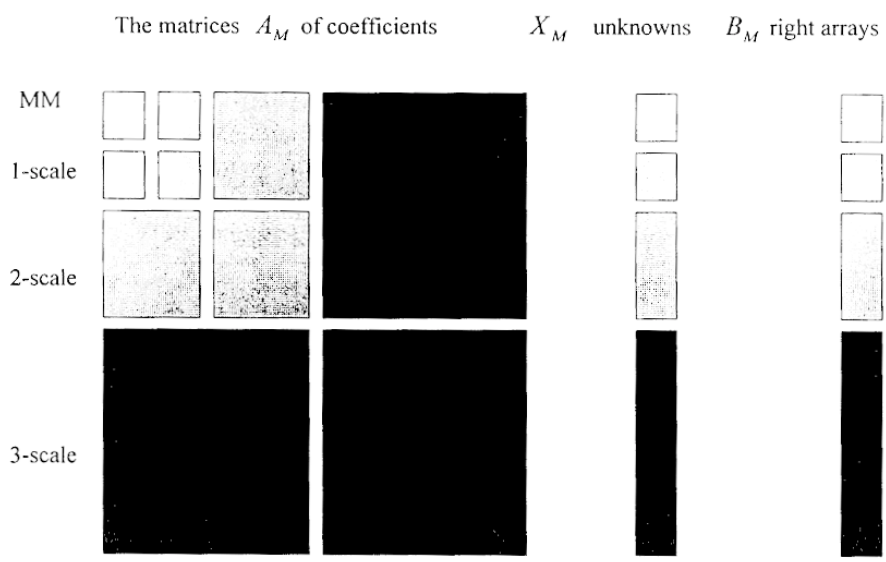

Figure 1. The illustration of coefficient matrices, the right arrays and the unknowns.

If we utilize the multiscale triangular basis functions using the moment method, then the matrix equation can be written as

$$A_M X_M = B_M \tag{11}$$

There are various relations between A, X, B and A_M, X_M, B_M. They are as follows:

$$A_M = TAT', \qquad B_M = TB, \qquad X = T'X_M$$

where T is the transformation matrix from the triangular basis to the multiscale triangular basis.

We should note that some elements of the solution X_M are zero or relatively smaller, particularly where the solution $X(v)$ is linear in some local interval. According to the characteristics of the expansion function through the use of multiscale triangular basis, we can omit these terms so as to reduce the size of the linear equations. The coefficient matrix A_M and the unknown X_M, and the source terms B_M are arranged in the form of the scaled-block (see Fig. 1) where MM denotes the block actually computed using the method of moments. The rest of the values are extrapolated.

The linear equation in (10) can be transformed to the linear equations of (11), through a matrix transformation and it has no relation with the

integral equation. Therefore, AMMM can be used for solving the matrix equation (7).

3.2 AMMM to Solve the Matrix Equation (7)

Although AMMM can be used directly to solve the matrix equation (7), some changes are needed because the current $\overline{J}_x$ and $\overline{J}_y$ have no relation between them. $\overline{J}_x$ and $\overline{J}_y$ can be expressed separately in the multiscale form, that is

$$\overline{J}_x = T'\overline{J}_x^M, \quad \overline{J}_y = T'\overline{J}_y^M$$

So the matrix equation (7) can be written in the following form as

$$\begin{pmatrix} A_{11}^M & A_{12}^M \\ A_{21}^M & A_{22}^M \end{pmatrix} \begin{pmatrix} \overline{J}_x^M \\ \overline{J}_y^M \end{pmatrix} = \begin{pmatrix} B_1^M \\ B_2^M \end{pmatrix} \tag{12}$$

where

$$A_{11}^M = TA_{11}T', \quad A_{12}^M = TA_{12}T', \quad A_{21}^M = TA_{21}T', \quad A_{22}^M = TA_{22}T'$$
$$B_1^M = \frac{4\pi}{jk\eta_0} T\overline{E}_x^i, \quad B_2^M = \frac{4\pi}{jk\eta_0} T\overline{E}_y^i$$

All of the matrices $A_{i,j}^M$, B_i^M are arranged in the form of the scaled-block like Fig. 1.

Because AMMM is based on solving the integral equation in one dimension, the unknowns in two dimension should be arranged in a certain sequence in order to solve the scattering from the plates in three dimension, that is, the center of the elements has to be arranged in a certain sequence. The unknown current vectors $\overline{J}_x$ and $\overline{J}_y$ can be viewed as the vectors constructed by the one-dimensional functions $J_x(l)$ and $J_y(l)$ at some discretized points $\{l_n\}$. The vector currents $\overline{J}_x^M$ and $\overline{J}_y^M$ can be considered as the coefficient vectors which $J_x(l)$ and $J_y(l)$ are for the multiscale triangular basis. Suppose the functions of $J_x(l)$ and $J_y(l)$ on V-scale are represented by $X_V^{J_x}(l)$ and $X_V^{J_y}(l)$, whose coefficients on the multiscale triangular basis are denoted by $\overline{X}_V^{J_x,J_y} = (\tau_{V,1}^{J_x,J_y}, \tau_{V,2}^{J_x,J_y}, \cdots, \tau_{V,2^{V-1}N}^{J_x,J_y})^T$ The procedure of solving the problem from a V-scale to a $(V+1)$-scale has four steps.

The first step is to predict the solution on $(V+1)$-scale from the known solution on V-scale by the interpolation method.

Between the unknown approximation functions on $(V+1)$-scale and the known approximation functions on V-scale, there is the following relation:

$$X_{V+1}^{J_x,J_y}(l) = X_V^{J_x,J_y}(l) + \sum_{i=1}^{2^V N} \tau_{V+1,i}^{J_x,J_y} \phi_{V+1,i}(l)$$

Hence, the known solution $X_V^{J_x J_y}(l)$ at the V-scale can be chosen as an initial guess for the unknown solution $X_{V+1}^{J_x,J_y}(l)$ for the $(V+1)$-scale if $\{\tau_{V+1,i}^{J_x,J_y}\}$ are set to be zero. However, $\tau_{V+1,i}^{J_x,J_y}$ can be estimated from $X_V^{J_x,J_y}(l)$ by the functional interpolation method (such as the polynomial interpolation, the spline interpolation, etc.), denoted as $X_{V+1}^{(0)J_x,J_y} = (\tau_{v+1,1}^{(0)J_x,J_y}, \tau_{v+1,2}^{(0)J_x,J_y}, \cdots, \tau_{V+1,2^V N}^{(0)J_x,Jy})^T$. Therefore, the initial guess for the array $(X_0^{J_x J_x}, X_1^{J_x,J_y}, \cdots, X_V^{J_x J_y}, X_{V+1}^{J_x J_y})$ can be constructed from the known array $(X_0^{J_x J_y}, X_1^{J_x,J_x}, \cdots, X_V^{J_x J_y})$ by the solution of the function $X_V^{J_x J_y}(l)$ and the array $X_{V+1}^{(0)J_x,J_y}$ can be estimated from $X_V^{J_x,J_y}(l)$ by the functional interpolation method.

The second step is to eliminate the relatively smaller components of the predicted solution components and omit the corresponding rows and columns from the system matrix obtained from the moment method. If $\left|\tau_{v,i}^{(0)J_x,J_y}\right| \leq \varepsilon$ ($v = 1, 2\cdots, V+1, i = 1, 2, \cdots, 2^v N$, ε is a given threshold), we set $\tau_{v,i}^{(0)J_x,J_y} = 0$, and omit the corresponding arrays and columns of the system matrix with respect to (v,i). This is an important step to reduce the size of the linear equation. In actual computation, we choose the following criterion $\left|\tau_{v,i}^{(0)J_x J_y}\right| \leq \varepsilon T^{J_x,J_y}$ ($T^{J_x} = \max\left|\tau_{v,i}^{(0)J_x}\right|$, $T^{J_y} = \max\left|\tau_{v,i}^{(0)J_y}\right|$).

The third step is to solve the modified linear equation after the above two steps by use of the Gauss method or the iterative methods.

The final step is to obtain the solution $(X_0^{J_x J_y}, X_1^{J_x,J_y}, \cdots, X_V^{J_x J_y}, X_{V+1}^{J_x,J_y})$ on the $(V+1)$-scale by adding some of the terms which have been eliminated by the second step.

The flow chart for solving the matrix equation utilizing the results from the V-scale to obtain the results for the $(V+1)$-scale is given in Fig. 2.

4. NUMERICAL RESULTS

In this section, we discuss some numerical examples for analyzing scattering from the perfectly conducting plates by use of AMMM. In the following

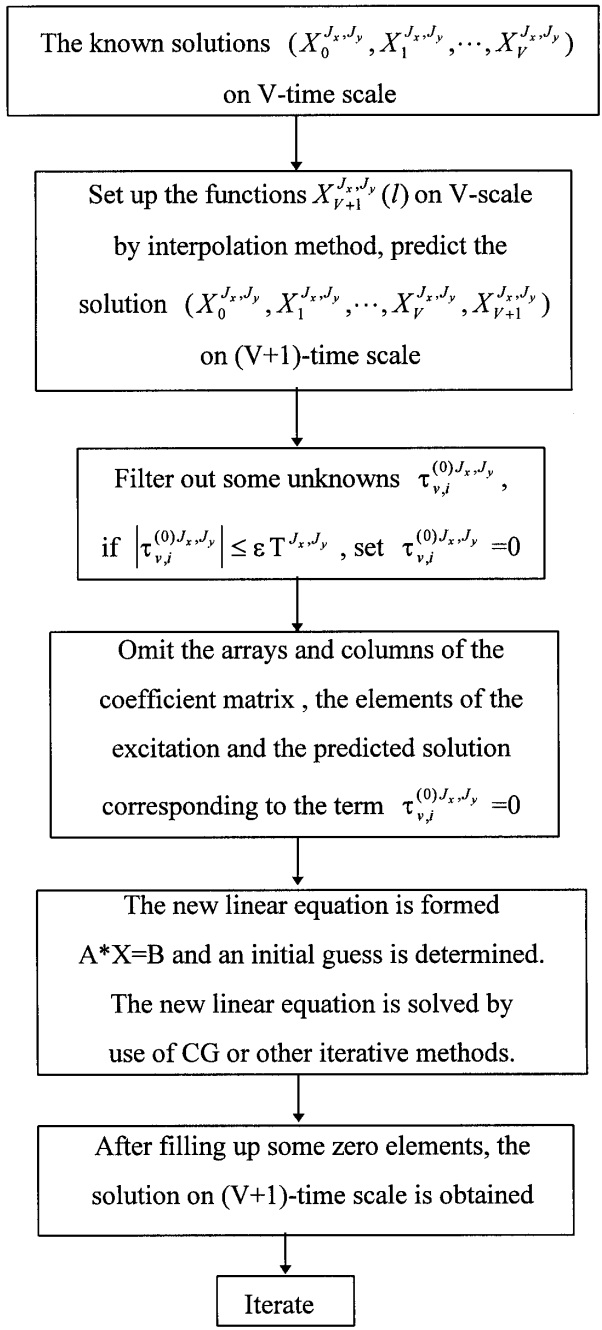

Figure 2. Flow chart of the adaptive multiscale moment method.

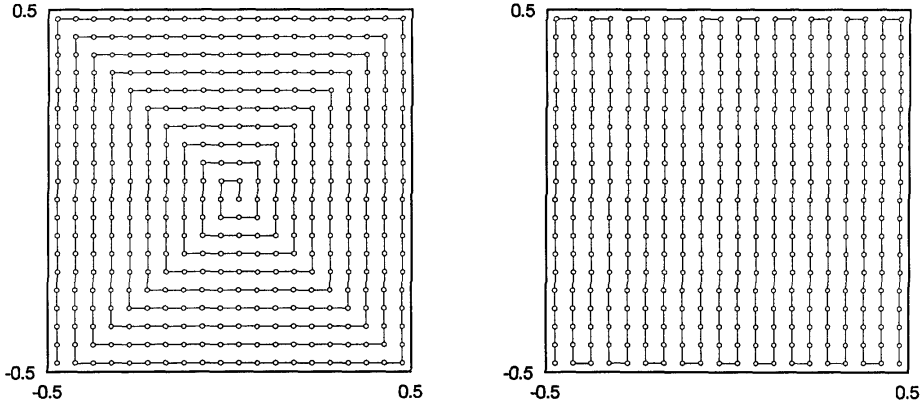

(a) The helix shape (b) The parallel shape

Figure 3. The center of elements is arranged in the helix and parallel shapes.

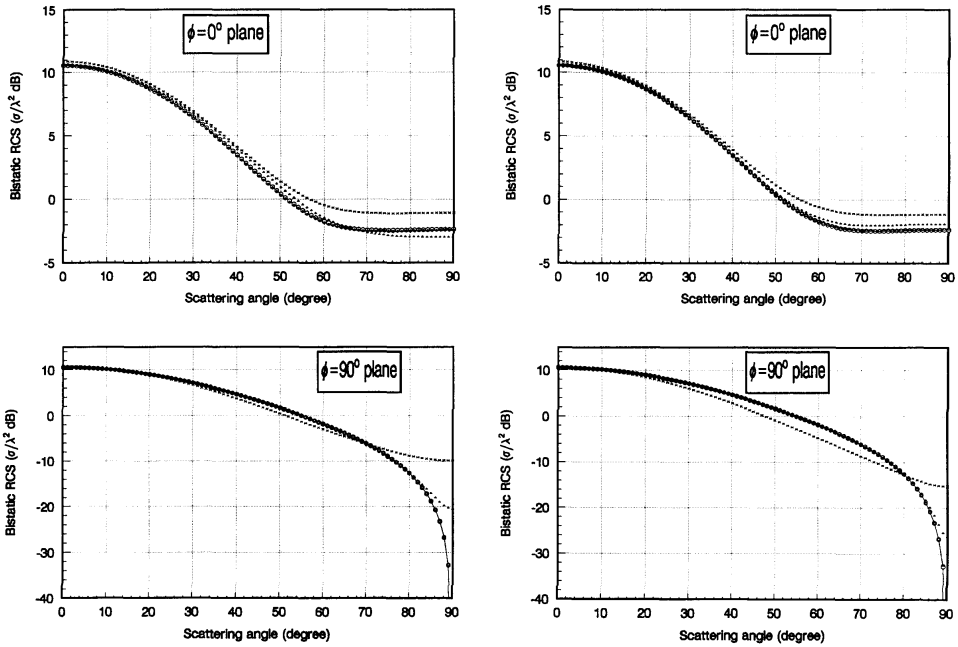

(a) The bistatic RCS for parallel arranged form (b) The bistatic RCS for Helix arranged form

Figure 4. The circle, square, triangle, and cross signals denote the results for the threshold $\varepsilon = 0, 0.01, 0.05, 0.1$. The Bistatic RCS on $\phi = 0°$ and $\phi = 90°$ for the two kind of arranged forms.

examples, the center of the elements is arranged in two different forms. One is the helix form, the other is the parallel form (see Fig. 3).

First example: consider the scattering from a $\mathbf{1}\lambda \times \mathbf{1}\lambda$ perfectly conducting plate. The plate is discretized into 20×20 cells. The center of the elements is arranged in two different forms as seen in Fig. 3. Total number of nodes is 400. Total unknowns for the linear equations are 800. The largest scale is taken as 3. So the number of unknowns for J_x and J_y is 50, 100, 200, 400 from 0-scale to 3-scale, respectively.

For the different thresholds and the arrangement of elements, the reduced number of J_x and J_y, the actual size of the linear equations, and the condition number on the 3-scale are given in the following table, when the conducting plate is illuminated by a normally incident plane wave with the magnetic field vector oriented along the $+y$ axis.

The condition numbers for the coefficient matrices for the helix arrangement form and the parallel arrangement form are 30140 and 26504, respectively. The bistatic RCS are shown in Fig. 4

Table 1

	The helix arrangement form			The parallel arrangement form		
Threshold	**0.01**	**0.05**	**0.1**	**0.01**	**0.05**	**0.1**
Reduced J_x	25	161	331	13	87	309
Reduced J_y	20	284	339	28	214	331
Actual size	755	355	150	759	499	160
Cond. No.	99334	7192	3075	123574	57894	7309

From table 1, it is shown that the smaller the threshold, the less the number of the unknowns that have been eliminated, and the larger is the condition number of the modified linear equation. When the threshold is taken 0.1, the size of the linear equation is reduced by about 81%, 80% respectively for the helix and parallel arrangement forms. And the errors of the bistatic RCS are admissible (see Fig. 4).

The monostatic RCS and the size of actual size of the linear equation on the 3-scale versus the angle of incidence with E-polarized and H-polarized plane wave are plotted in Fig. 5.

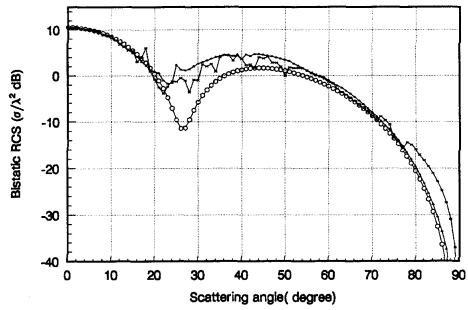

(a) The monostatic RCS and the size of the linear equation for V-polarized plane wave

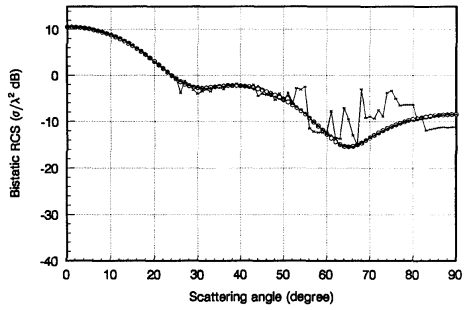

(b) The monostatic RCS and the size of the linear equation for H-polarized plane wave

Figure 5. The circle, triangle, and cross signals denote the results for the threshold $\varepsilon = 0, 0.01, 0.05$. The monostatic RCS and size of the linear equation for V-polarized and H-polarized plane wave.

Second example: consider the scattering from a $\mathbf{2}\lambda \times \mathbf{2}\lambda$ perfectly conducting plate. The plate is discretized into 20×20 cells. The center of the cells is arranged in the same two different forms which have been explained for the first example. Total number of nodes is 400. Total number of unknowns for the linear equations is 800.

For the different thresholds and arrangement cells, the reduced number of J_x and J_y the actual size of the linear equations, and condition number on the 3-scale are given in the following table, when the conducting plate is illuminated by a normally incident plane wave with the magnetic field vector oriented along the $+y$ axis.

The condition numbers of coefficient matrices for the helix arrangement form and the parallel arrangement form are 2874 and 2123, respectively. The bistatic RCS has been shown in Fig. 6.

Table 2

	The helix arrangement form			The parallel arrangement form		
Threshold	**0.01**	**0.05**	**0.1**	**0.01**	**0.05**	**0.1**
Reduced J_x	3	192	288	3	155	294
Reduced J_y	9	153	290	3	152	324
Actual size	788	455	222	794	493	182
Cond. No.	87184	84538	3372	26331	13594	2581

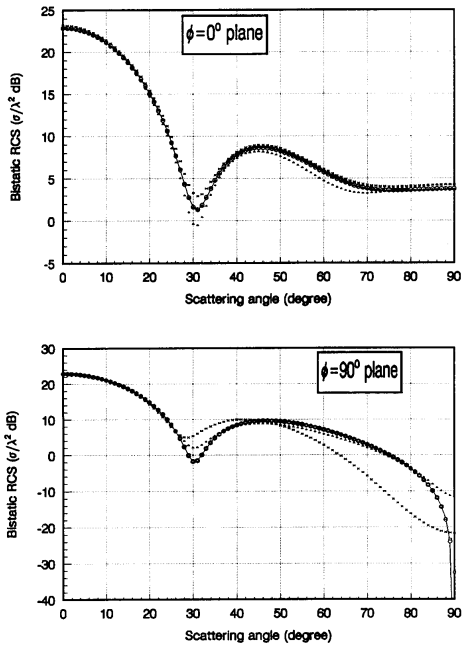

(a) The bistatic RCS for parallel arranged form

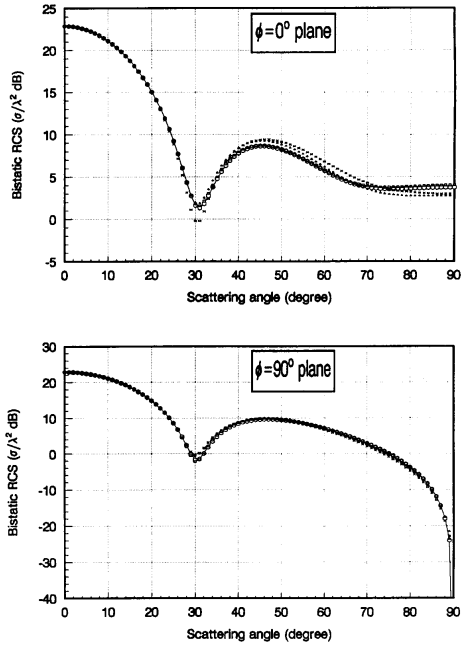

(b) The bistatic RCS for Helix arranged form

Figure 6. The circle, square, triangle, and cross signals denote the results for the threshold $\varepsilon = 0, 0.01, 0.05, 0.1$. The Bistatic RCS on $\phi = 0°$ and $\phi = 90°$ for the two kind of arranged forms.

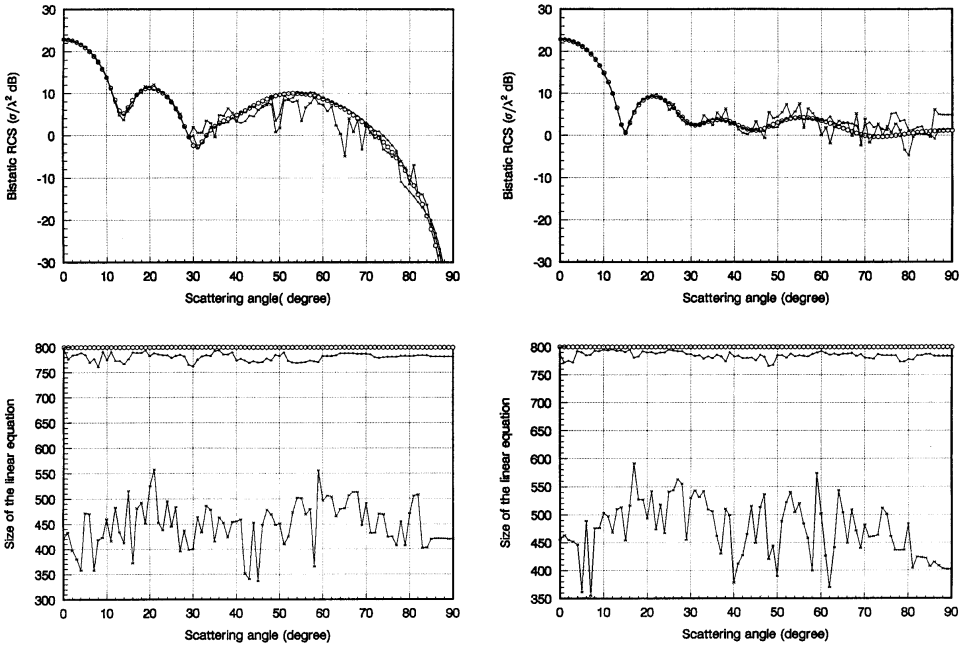

(a) The monostatic RCS and the size of the linear equation for V-polarized plane wave

(b) The monostatic RCS and the size of the linear equation for H-polarized plane wave

Figure 7. The circle, triangle, and cross signals denote the results for the threshold $\varepsilon = 0, 0.01, 0.05$. The monostatic RCS and size of the linear equation for V-polarized and H-polarized plane wave.

The monostatic RCS and the size of actual size of the linear equation on the 3-scale versus the angle of incidence with E-polarized and H-polarized plane wave are plotted in Fig. 7.

Third example: consider the scattering from a $\mathbf{2}\lambda \times \mathbf{3}\lambda$ perfectly conducting plate on the x-y plane (the length on x-axis is $\mathbf{2}\lambda$, the length on the y-axis is $\mathbf{3}\lambda$). The plate is discretized into 20×30 cells. The center of the cells is arranged in the helix form. Total number of nodes is 600. Total number of unknowns in the linear equations is 1200. The largest scale is taken to be 3. So the number of unknowns for J_x and J_y is 75, 150, 300, 600 from 0-scale to 3-scale, respectively.

Fig. 8 shows the monostatic RCS and the size of the actual size of the linear equation on the 3-scale versus the angle of incidence plane wave with the magnetic field vector oriented along the $+y$ axis on $\phi = 0$ plane.

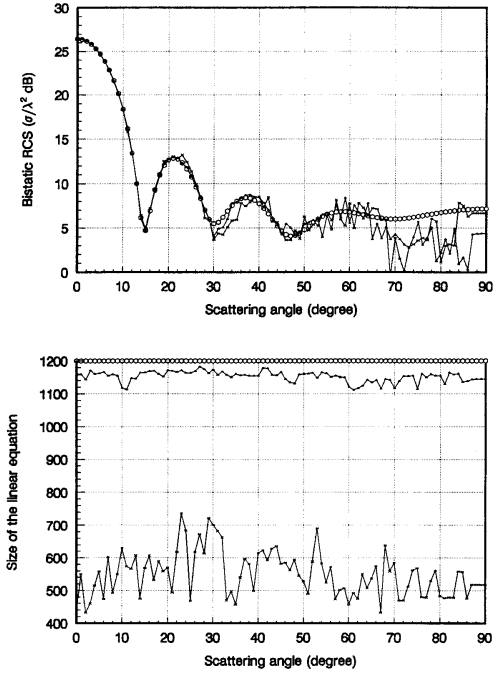

Figure 8. The circle, triangle, and cross signals denote the results for the threshold $\varepsilon = 0, 0.01, 0.05$. The monostatic RCS and size of the linear equation for H-polarized plane wave.

5. CONCLUSIONS

AMMM has been used to analyze scattering from the perfectly conducting plates. By use of the matrix transformation, the impedance matrix and the source terms constructed by the conventional moment method can be arranged in the form of different scales. From one scale to another scale, the initial guess can be predicted according to the properties of the multiscale technique. Some examples have been presented that clearly shows that AMMM can reduce adaptively the size of the linear equations and can improve the efficiency over that of the conventional moment method. Although the pulse basis and point-matching technique is adapted in this paper, the AMMM can be used to improve the efficiency when other basis functions (such as the rooftop functions, Rao's basis functions) are chosen in the moment method to study the scattering problems. The extension of this technique to three dimensional case is underway and the results will be reported in due time.

REFERENCES

1. Harrington, R. F., *Field Computation by Moment Method,* Hacmillan Press, New York,1968.
2. Miller, E. K., L. Medgyesi-Mitschang, and E. H. Newman, Eds., *Computational Electromagnetics: Frequency-Domain Method of Moments,* New York: IEEE Press, 1992.
3. Bouche, D. P., F. A. Molinet, and R. Mittra, "Asymptotic and hybrid techniques for electromagnetic scattering," *Proc. IEEE,* Vol. 81, No. 12, 1658–1684, Dec. 1993.
4. Thiele, G. A., "Overview of selected hybrid method in radiating system analysis," *Proc. IEEE,* Vol. 80, No. 1, 67–78, Jan. 1992.
5. Medgyesi-Mitschang, L. N., and D. S. Wang, "Hybrid methods in computational electromagnetics: A review," *Computer Physics Communications,* Vol. 68, 76–94, May 1991.
6. Canning, F. X., "The impedance matrix localization method (IML) uses," *IEEE AP,* Vol. 41, No. 5, 1659–667, 1993.
7. Canning, F. X., "The impedance matrix localization method (IML) permits solution of large scatterers," *IEEE Magnetics,* Vol. 27, 4275–4277, Sept. 1991.
8. Canning, F. X., "The impedance matrix localization method (IML) for MM calculation," *IEEE AP Magazine,* Vol. 32, l8–30, Oct. 1990.
9. Canning, F. X., "Transformations that produce a sparse moment method matrix," *J. Electromag. Wave Applicat.,* Vol. 4, No. 9, 893–913, 1990.
10. Coifman, R., V. Rohklin, and S. Wandzura, "The fast multipole method for the wave equation: A pedestrian prescription," *IEEE Antennas Propagat. Mag.,* Vol. 35, 7–12, 1993.
11. Rohklin, V., "Rapid solution of integral equations of scattering in two dimensions," *J. Comput. Phys.,* Vol. 86, 414–439, 1990.
12. Rohklin, V., "Rapid solution of integral equations of classical potential theory," *J. Comput. Phys.,* Vol. 60, 187–207, 1985.
13. Boag, A., and R. Mittra, "Complex multipole beam approach to electromagnetic scattering problems," *IEEE Trans. Antennas Propagat.,* Vol. AP-42, 366–372, Mar. 1994.
14. Michielssen, E., and A. Boag, "Multilevel evaluation of electromagnetic fields for the rapid solution of scattering problems," *Microwave Opt. Tech. Lett.,* Vol. 7, No. 17, 790–795, Dec. 1994.
15. Michielssen, E., and A. Boag, "A multilevel matrix decomposition algorithm for analyzing scattering from large structures," *11th Annu. Rev. Progress ACES, Monterey, CA,* 614–620, Mar. 1995.
16. Michielssen, E., and A. Boag, "A multilevel matrix decomposition algorithm for analyzing scattering from large structures", *IEEE Trans. Antennas Propagat.,* Vol. AP-44, No. 8, 1086–1093, Aug. 1996.

17. Chew, W. C., J. M. Jin, C. C. Lu, E. Michielssen, and J. M. Song, "Fast solution methods in electromagnetics," *IEEE Trans. Antennas Propagat.*, Vol. AP-45, no. 3, 533–543, Mar. 1997.
18. Su, Chaowei, and T. K. Sarkar, "A multiscale moment method for solving Fredholm integral equation of the first kind," *J. Electromag. Waves Appl.,* Vol. 12, 97–101, 1998.
19. Su, Chaowei, and T. K. Sarkar, "Electromagnetic scattering from coated strips utilizing the adaptive multiscale moment method," *Progress In Electromagnetics Research,* PIER 18, 173–208, 1998.
20. Su, Chaowei, and T. K. Sarkar, "Electromagnetic scattering from two-dimensional electrically large perfectly conducting objects with small cavities and humps by use of adaptive multiscale moment methods (AMMM)," *J. Electromag. Waves Appl.,* Vol. 12, 885–906, 1998.
21. Mittra, R., Y. Rahmat-Samii, D. V. Jamnejad, and W. A. Davis, "A new look at the thin-plate scattering problem," *Rad. Sci.,* Vol. 8, No. 10, 869–875, Oct. 1973.
22. Rahmat-Samii, Y., and R. Mittra, "Integral equation solution and RCS computation of a thin rectangular plate," *IEEE Trans. Antennas Propagat.,* Vol. AP-22, No. 7, 608–610, July 1974.
23. Tran, T. V., and A. McCowen, "An improved pulse-basis conjugate gradient FFT method for the thin conducting plate problem," *IEEE Trans. Antennas Propagat.,* Vol. AP-41, No. 2, 185–189, Feb. 1993.
24. Peters, T. J., and J. L. Volakis, "Application of a conjugate gradient FFT method to scattering from thin planar material plates," *IEEE Trans. Antennas Propagat.,* Vol. 36, No. 4, 518–526,Apr. 1988.
25. Barkeshli, K., and J. L. Volakis, "On the implementation of the conjugate gradient Fourier transform method for scattering by planar plates," *IEEE Trans. Antennas Propagat. Mag.,* Vol. 32, 19–29, Apr. 1990.
26. Catedra, M. F., J. G. Cuevas, and L. Nuno, "A scheme to analyze conducting plates of resonant size using the conjugate gradient method and the fast Fourier transform," *IEEE Trans. Antennas Propagat.,* Vol. AP-36, No. 12, 1744–1752, Dec. 1988.
27. Shen, C. Y., K. J. Glover, M. I. Sancer, and A. D. Varvatsis, "The discrete Fourier transform method of solving different-integral equations in scattering theory," *IEEE Trans. Antennas Propagat.,* Vol. AP-37, No. 8, 1032–1041, Aug. 1988.
28. Zhamborn, A. P. M., and P. M. van den Berg, "A weak form of the conjugate gradient FFT method for plate problems," *IEEE Trans. Antennas Propagat.,* Vol. AP-39, No. 2, 224–228, Feb. 1991.